HEAT TRANSFER CALCULATIONS OF NON-DEVELOPED STEADY LAMINAR FLOW BETWEEN PARALLEL PLATES

T. A. Al-Hattab, A. A. Al-Moosawy, and A. A. Shaker
Babylon University, College of Engineering

ABSTRACT
The objective of the current research is to investigate the developing laminar flow of a Newtonian incompressible fluid and heat transfer in the entrance region of a two parallel plate channel were investigated. The continuity, x-momentum, and energy equations were solved as a steady state in two dimension equations. The dimensionless technique was used. These equations have been represented by finite difference technique. This model has been solved by using the new method of implicit scheme, which would minimize the solution errors. The velocity profile becomes fully developed at approximately $L_e/2a = 0.05\,Re$, and the temperature distribution becomes fully developed at approximately $L_{et}/2a = 0.05\,Re\,.\,Pr$, as expected. The computational algorithm is able to calculate all the hydrodynamic properties such as velocities. Also the computational algorithm is able to predict all the thermal properties such as the temperature, bulk temperature, and local Nusselt number. The validity of thermal results for constant wall temperature and constant wall heat flux is verified and shows that there is a good agreement between the results of the present numerical solution and the correlation related to it.

Keywords: Entrance Region, Laminar Flow, Steady, Parallel Plates

حسابات انتقال الحرارة للجريان الطبائقي المستقر المتطوِّر بين صفيحتين متوازيتين

تحسين علي الحطاب ، عادل عباس الموسوي ، أحمد علي شاكر

الخلاصة

الهدف من البحث الحالي هو دراسة الجريان الطبائقي غير تام التطوّر لمائع غير قابل للانضغاط (يخضع لقوانين نيوتن) وانتقال الحرارة لمنطقة النمو خلال مجرى متكون من صفيحتين متوازيتين. تم الحل لمعادلة الاستمرارية و معادلة الزخم باتجاه المحور السيني و معادلة الطاقة للحالة المستقرة ذات البعدين. تم استخدام تقنية الحل اللابعدي. هذه المعادلات مُثلت بتقنية الفروقات المحددة. هذا النموذج حُلَّ باستخدام طريقة جديدة، التي تقلل من أخطاء الحل. شكل توزيع السرع يصبح كامل النمو عند حوالي ($L_e/2a = 0.05\,Re$) وشكل توزيع درجات الحرارة يصبح كامل النمو عند حـوالي ($L_{et}/2a = 0.05\,Re\,.\,Pr$)، كمـا متوقـع. إمكانيـة الحـل العـددي تتـضمن حـساب جميـع الـصفات الهيدروديناميكية مثل منحنيات السرعة، و كذلك تتضمن إمكانية الحل العددي القدرة على تنبؤ جميع الصفات الحرارية مثل توزيع درجات الحرارة و متوسط درجة الحرارة و رقم نسلت الموضعي. تم التأكد من صحَّة النتائج الحرارية لحالة التسخين بثبوت درجة حرارة الجدار و ثبوت الفيض الحراري للجدار حيث كان هنالك توافق جيد بين الحل العددي الحالي والعلاقات التجريبية و النظرية المتعلقة به الباحثين سابقين.

INTRODUCTION

Heat transfer in the combined entry region of non-circular ducts is of particular interest in the design of compact heat exchangers. In these applications passages are generally short and usually composed of cross-sections such as triangular or rectangular geometries in addition to the circular tube or parallel plate channel. Also, due to the wide range of applications, fluid prandtl numbers usually vary between (0.1 < Pr < 1000), which covers a wide range of fluids encompassing gases and highly viscous liquids such as automotive oils.

Closed form solutions do not exist for the problem, hydrodynamically and thermally developing laminar flow between two parallel plates. Thus, this problem can be solved by using numerical methods. A numerical solution is obtained by considering the momentum and energy equations and the continuity equation. The solution presented here is an attempt to provide a complete picture of the hydrodynamic and thermal variation in the flow within the entire channel.

Laminar flow solution for entrance region non-isothermal flow and heat transfer to power-law fluids with rectangular coordinates transformed into new orthogonal coordinates and the finite difference technique for arbitrary cross-section ducts were studied by Lawal (1989). Al-Ali and Selim (1992) studied developing laminar flow and heat transfer in the entrance region of a parallel plate channel with uniform surface temperature by a new integral method. Unlike earlier Karman-Pohlhausen analyses, the new analysis provides solutions which are free from jump discontinuities in the gradients of the velocity and temperature distributions throughout and at the end of the entrance region. The hydrodynamic and thermal results from the present analysis therefore join smoothly and asymptotically to their fully- developed values. The heat transfer results obtained are further found to agree well with previously published numerical solutions. Lakovic, Stefanovic, Ilic, and Stojiljkovic (1997) investigated convective heat and mass transfer in the part of hydrodynamic stabilization of the flow through the channel formed of two parallel plates. The solution is given for the boundary conditions of the first kind. The similarity method between this problem and corresponding potential flow is applied, in order to obtain the solution. Silva, Guerrero, and Cotta (1999) studied the boundary layer equations for steady incompressible laminar channel flow by integral transform method, adopting the stream function-only formulation of the governing equations, instead of the more commonly used primitive variables formulation. This hybrid numerical-analytical approach provides benchmark results under user-prescribed accuracy targets and is recognized in the validation of purely numerical schemes. The relative merits of the stream function formulation are illustrated through numerical results for the convergence behavior in the case of a plane Poiseuille flow. Adachi and Uehara (2001) investigated the correlation between heat transfer and pressure drop in channels with periodically grooved parts along the streamwise direction for various channel configurations by assuming two-dimensional and periodically fully developed flow and temperature fields. Streamwise periodic variations of the cross-section induce the bifurcation from steady-state flow to oscillatory one. Heat transfer is enhanced significantly after the bifurcation with the increase of pressure drop. An efficiency defined as the ratio of the heat transfer enhancement to the increase of pressure drop is considered. It is found that the channels with expanded grooves perform efficiently while the channels with contracted grooves inefficiently. Barber and Emerson (2002) studied the role of the Reynolds number on the hydrodynamic development length at the entrance to parallel plate micro-channels. The entrance

development region is almost 25% longer than that predicted using continuum flow theory.

MATHEMATICAL MODEL

The mathematical analysis is presented for the Partial Differential Equations which describe developing laminar fluid flow and heat transfer in parallel plate channel. Incompressible and constant property flow is assumed for developing velocity and temperature profile in the entrance region of the two parallel plates channel. The parallel plate channel has been chosen for initial consideration because the formulation illustrates the techniques used for confined flows without the complicating geometrical and three-dimensional factors of other configurations.

Assumptions

The parallel plate channel will be expressed in Cartesian Coordinates System. This study will be achieved for two cases, Constant Wall Temperature and Constant Heat Flux respectively. For two dimensional developing, steady state, incompressible laminar flow in parallel plate channel the effects of heat conduction, body force, free convection, heat generation and viscous dissipation within the fluid are neglected.

Governing Equations

The following formulation is based largely on the work of Bodoia and Osterle [mentioned by Hornbeck, 1973] and [Incropera, 1996]. The equations of motion are assumed to be

Continuity equation:

$$\frac{\partial u}{\partial x} + \frac{\partial v}{\partial y} = 0 \tag{1}$$

x-momentum equation:

$$u\frac{\partial u}{\partial x} + v\frac{\partial u}{\partial y} = -\frac{1}{\rho}\frac{dp}{dx} + v\frac{\partial^2 u}{\partial y^2} \tag{2}$$

Equation (2) is the x-component of momentum equation for a steady, two dimensional, laminar, constant-property boundary-layer flow of a Newtonian fluid in forced convection. The two terms on the left hand side are the nonlinear convection terms. The two terms on the right hand side arise from inertial forces and viscous shearing forces, respectively.

The energy equation for incompressible, constant property flow is uncoupled from the momentum equation once the velocity distribution is known. When viscous dissipation is neglected, the energy equation may be written as

Energy equation:

$$u\frac{\partial T}{\partial x} + v\frac{\partial T}{\partial y} = \alpha\frac{\partial^2 T}{\partial y^2} \tag{3}$$

The Dimensionless Quantities

Before undertaking a numerical solution, the first step should invariably place the equations to be solved in a dimensionless form having as few parameters as possible. This may be accomplished for equations (1), (2) and (3) by employing the following dimensionless variables :-

$$\left.\begin{array}{l} U = \dfrac{u}{u_o} \\[2mm] V = \dfrac{v}{u_o} \\[2mm] X = \dfrac{x}{d} \\[2mm] Y = \dfrac{y}{d} \\[2mm] P = \dfrac{p}{\rho u_o^2} \end{array}\right\} \qquad (4)$$

For the Constant wall temperature, the thermal boundary condition will be:

$$\theta = \frac{T - T_w}{T_o - T_w} \qquad (5)$$

For the Constant wall heat flux, the thermal boundary condition will be:

$$\theta = \frac{k}{qd}\left(T - T_o\right) \qquad (6)$$

The following dimensionless quantities will be used in the present work:
Reynolds number:

$$\mathrm{Re} = \frac{\rho.u_o.d}{\mu} \qquad (7)$$

Prandtl number:

$$\mathrm{Pr} = \frac{c_p \mu}{k} = \frac{v}{\alpha} \qquad (8)$$

Nusselt number:

$$Nu = \frac{h.d}{k} \qquad (9)$$

Dimensionless Governing Equations
The continuity equation may be made dimensionless by the choice of the dimensionless variables shown in equation (4):
<u>**Continuity equation:**</u>

$$\frac{\partial U}{\partial X} + \frac{\partial V}{\partial Y} = 0 \qquad (10)$$

The x-momentum equation may be made dimensionless by the choice of the dimensionless variables of (4) and (7):
<u>**X-momentum equation:**</u>

$$U\frac{\partial U}{\partial X} + V\frac{\partial U}{\partial Y} = -\frac{\partial P}{\partial X} + \frac{1}{\mathrm{Re}}\frac{\partial^2 U}{\partial Y^2} \qquad (11)$$

The energy equation for constant wall temperature may be made dimensionless by the choice of the dimensionless variables of (4), (5), (7) and (8) and for constant heat flux (4), (6), (7) and (8):

Energy equation:

$$U \frac{\partial \theta}{\partial X} + V \frac{\partial \theta}{\partial Y} = \frac{1}{\Pr . \mathrm{Re}} \frac{\partial^2 \theta}{\partial Y^2} \qquad (12)$$

Boundary Conditions

The boundary conditions may be made dimensionless by the choice of the dimensionless variables (4), (5) and (6):

Entrance region Dimensionless Boundary Conditions:

Uniform temperature and velocity profile at the entrance region of parallel plate channel is assumed. All entrance boundary conditions can be written as follows [Hornbeck, 1973]:

$$\left. \begin{array}{l} U(0,Y) = 1 \\ V(0,Y) = 0 \\ P(0) = 1 \end{array} \right\} \qquad (13)$$

For the Constant wall temperature, the thermal boundary condition will be:

$$\theta(0,Y) = 1 \qquad (14)$$

For the Constant wall heat flux, the thermal boundary condition will be:

$$\theta(0,Y) = 0 \qquad (15)$$

Wall Dimensionless Boundary Conditions:

All dimensionless velocity components are zero at walls, hence:

$$\left. \begin{array}{l} U(X,1) = 0 \\ V(X,1) = 0 \end{array} \right\} \qquad (16)$$

A number of dimensionless temperature boundary conditions at the wall are possible:
For the Constant wall temperature, the thermal boundary condition will be:

$$\theta(X,1) = 0 \qquad (17)$$

For the Constant wall heat flux, the thermal boundary condition will be:

$$\frac{\partial \theta}{\partial Y}(X,1) = 1 \qquad (18)$$

Centerline of duct dimensionless Boundary Conditions:

At centerline of the duct the dimensionless boundary conditions are:

$$\left. \begin{array}{l} \frac{\partial U}{\partial Y}(X,0) = 0 \\ V(X,0) = 0 \\ \frac{\partial \theta}{\partial Y}(X,0) = 0 \end{array} \right\} \qquad (19)$$

Bulk Temperature

In order to solve for the heat transfer in confined flow situation, it is first necessary to find the bulk (mixed-mean) temperature. This quantity is defined for the parallel plate channel as

$$T_b \equiv \frac{\int_0^a u.T.dy}{\int_0^a u.dy} \tag{20}$$

The dimensionless bulk temperature is

$$\theta_b \equiv \frac{\int_0^1 U.\theta.dY}{\int_0^1 U.dY} \tag{21}$$

Dimensionless Bulk Temperature:

$$\theta_b = \frac{\int_0^1 U.\theta.dY}{\int_0^1 U.dY} = \int_0^1 U.\theta.dY \tag{22}$$

$$where \int_0^1 U.dY = 1$$

Local Nusselt Number

$$N_{ux} = \frac{2ha}{k} \tag{23}$$

where

$$h(T_w - T_b) = k\frac{\partial T}{\partial y}\bigg|_{y=a} \tag{24}$$

so

$$N_{ux} = \frac{-\frac{\partial T}{\partial y}\bigg|_{y=a}(2a)}{T_b - T_w} \tag{25}$$

The dimensionless variables for constant wall temperature boundary condition are:

$$\left.\begin{aligned} \theta &= \frac{T - T_w}{T_o - T_w} \\ Y &= \frac{y}{a} \end{aligned}\right\} \tag{26}$$

The dimensionless local Nusselt Number for constant wall temperature:

$$N_{ux} = \frac{-2\frac{\partial \theta}{\partial Y}\Big|_{Y=1}}{\theta_b} \tag{27}$$

The dimensionless variables for constant wall heat flux boundary condition are:

$$\left.\begin{array}{l} \theta = \dfrac{k}{q.a}(T - T_o) \\[2ex] Y = \dfrac{y}{a} \end{array}\right\} \tag{28}$$

The dimensionless local Nusselt Number for constant wall heat flux:

$$N_{ux} = \frac{-2}{\theta_b - \theta_w} \tag{29}$$

Numerical Formulation for Momentum and and Continuity Equations
The special Finite Difference Method will be used to solved the momentum equation for a steady, two-dimensional, laminar, constant-property boundary-layer flow of a Newtonian fluid in forced convection. The two terms on the left side are the nonlinear convection terms. The two terms on the right side arise from inertial forces and viscous shearing forces, respectively. The numerical formulation for x-momentum equation is [Hornbeck, 1973]

$$U_{i,j}\frac{U_{i+1,j} - U_{i,j}}{\Delta X} + V_{i,j}\frac{U_{i+1,j+1} - U_{i+1,j-1}}{2(\Delta Y)} = -\frac{P_{i+1} - P_i}{\Delta X} + \frac{1}{\text{Re}}\frac{U_{i+1,j+1} - 2U_{i+1,j} + U_{i+1,j-1}}{(\Delta Y)^2} \tag{30}$$

A somewhat unusual representation of equation (10) is chosen for a reason which will become clear shortly. The form is

$$\frac{U_{i+1,j+1} - U_{i,j+1} + U_{i+1,j} - U_{i,j}}{2(\Delta X)} + \frac{V_{i+1,j+1} - V_{i+1,j}}{\Delta Y} = 0 \tag{31}$$

Equations (30) and (31) are written for j=0(1)n constitute (*2n+2*) equations in the (*2n+2*) unknowns ($U_{i+1,0},....,U_{i+1,n}$; $V_{i+1,1},....,V_{i+1,n}$); and (P_{i+1}). The number of unknowns can be reduced materially by writing the continuity equation (31) for j=0(1)n and adding together all of these equations. The resulting equation is

$$U_{i+1,0} + 2\sum_{j=1}^{n} U_{i+1,j} = U_{i,0} + 2\sum_{j=1}^{n} U_{i,j} \tag{32}$$

Since equation (32) does not involve (*V*), equation (32) together with equation (30) written for j=0(1)n now constitute (*n+2*) equations in the (*n+2*) unknowns ($U_{i+1,0},....,U_{i+1,n}$) and (P_{i+1}). To aid in obtaining a solution, it is convenient to rewrite equation (30) as

$$\left[\frac{-V_{i,j}}{2(\Delta Y)} - \frac{1}{\text{Re}(\Delta Y)^2}\right]U_{i+1,j-1} + \left[\frac{U_{i,j}}{\Delta X} + \frac{2}{\text{Re}(\Delta Y)^2}\right]U_{i+1,j} + \left[\frac{V_{i,j}}{2(\Delta Y)} - \frac{1}{\text{Re}(\Delta Y)^2}\right]U_{i+1,j+1} + \left[\frac{1}{\Delta X}\right]P_{i+1} = \frac{U_{i,j}^2 + P_i}{\Delta X}$$

(33)

Equations (33) [written for j=0(1)n] and (32) may be written in matrix form as

$$
\begin{vmatrix}
1 & 2 & 2 & 2 & 2 & - & - & 2 & 2 & 0 \\
\beta_0 & \Omega_0 & & & & & & & & 1/\Delta X \\
\varepsilon_1 & \beta_1 & \Omega_1 & & & & & & & 1/\Delta X \\
& \varepsilon_2 & \beta_2 & \Omega_2 & & & & & & 1/\Delta X \\
& & \varepsilon_3 & \beta_3 & \Omega_3 & & & & & 1/\Delta X \\
& & & - & - & - & & & & - \\
& & & & - & - & - & & & - \\
& & & & - & - & - & & & - \\
& & & & & \varepsilon_{n-1} & \beta_{n-1} & \Omega_{n-1} & & 1/\Delta X \\
& & & & & & \varepsilon_n & \beta_n & & 1/\Delta X
\end{vmatrix}
\times
\begin{vmatrix}
U_{i+1,0} \\
U_{i+1,1} \\
U_{i+1,2} \\
U_{i+1,3} \\
U_{i+1,4} \\
- \\
- \\
- \\
U_{i+1,n} \\
P_{i+1}
\end{vmatrix}
=
\begin{vmatrix}
S \\
\Phi_0 \\
\Phi_1 \\
\Phi_2 \\
\Phi_3 \\
- \\
- \\
- \\
\Phi_{n-1} \\
\Phi_n
\end{vmatrix}
\quad (34)
$$

where

$$\Omega_0 = -\frac{2}{\mathrm{Re}(\Delta Y)^2} \qquad (incorporates\ symmetry\ at\ Y=0) \tag{35}$$

$$S = U_{i,0} + 2\sum_{j=1}^{n} U_{i,j} \tag{36}$$

and

$$\varepsilon_j = -\frac{V_{i,j}}{2(\Delta Y)} - \frac{1}{\mathrm{Re}(\Delta Y)^2} \tag{37}$$

$$\beta_j = \frac{U_{i,j}}{\Delta X} + \frac{2}{\mathrm{Re}(\Delta Y)^2} \tag{38}$$

$$\Omega_j = \frac{V_{i,j}}{2(\Delta Y)} - \frac{1}{\mathrm{Re}(\Delta Y)^2} \quad (j > 0) \tag{39}$$

$$\Phi_j = \frac{U_{i,j}^2 + P_i}{\Delta X} \tag{40}$$

After the set (34) has been solved for $(U_{i+1,0},\ldots,U_{i+1,n})$ and (P_{i+1}), equation (31) may be employed in the form

$$V_{i+1,j+1} = V_{i+1,j} - \frac{\Delta Y}{2(\Delta X)}\left(U_{i+1,j+1} - U_{i,j+1} + U_{i+1,j} - U_{i,j}\right) \tag{41}$$

which may be marched outward from the channel centerline to give the values of $(V_{i+1,1},\ldots,V_{i+1,n})$.

Numerical Formulation for Energy Equation
Equation (12) may now be expressed in an implicit finite difference form similar to that used for the momentum equation in the preceding section. This difference form is

$$U_{i,j}\frac{\theta_{i+1,j} - \theta_{i,j}}{\Delta X} + V_{i,j}\frac{\theta_{i+1,j+1} - \theta_{i+1,j-1}}{2(\Delta Y)} = \frac{1}{\mathrm{Pr.Re}}\frac{\theta_{i+1,j+1} - 2\theta_{i+1,j} + \theta_{i+1,j-1}}{(\Delta Y)^2} \tag{42}$$

Equation (42) can be rewritten in a more useful form as

$$\left[\frac{-V_{i,j}}{2(\Delta Y)} - \frac{1}{\mathrm{Pr.Re}(\Delta Y)^2}\right]\theta_{i+1,j-1} + \left[\frac{U_{i,j}}{\Delta X} + \frac{2}{\mathrm{Pr.Re}(\Delta Y)^2}\right]\theta_{i+1,j} + \left[\frac{V_{i,j}}{2(\Delta Y)} - \frac{1}{\mathrm{Pr.Re}(\Delta Y)^2}\right]\theta_{i+1,j+1} = \frac{U_{i,j}\theta_{i,j}}{\Delta X} \tag{43}$$

Equation (43) is written for j=0(1)n forms as a set of (*n+1*) simultaneous linear equations in the values of $(\theta_{i+1,j})$. If the wall temperature is known (Constant Wall

Temperature case), then these $(n+1)$ equations involve $(n+1)$ unknowns. The resulting matrix equation is

$$
\begin{vmatrix}
\beta'_0 & \Omega'_0 & & & & & \\
\varepsilon'_1 & \beta'_1 & \Omega'_1 & & & & \\
& \varepsilon'_2 & \beta'_2 & \Omega'_2 & & & \\
& & - & - & - & & \\
& & & - & - & - & \\
& & & & - & - & - \\
& & & & \varepsilon'_{n-1} & \beta'_{n-1} & \Omega'_{n-1} \\
& & & & & \varepsilon'_n & \beta'_n
\end{vmatrix}
\times
\begin{vmatrix}
\theta_{i+1,0} \\
\theta_{i+1,1} \\
\theta_{i+1,2} \\
- \\
- \\
- \\
\theta_{i+1,n-1} \\
\theta_{i+1,n}
\end{vmatrix}
=
\begin{vmatrix}
\Phi'_0 \\
\Phi'_1 \\
\Phi'_2 \\
- \\
- \\
- \\
\Phi'_{n-1} \\
\Phi'_n
\end{vmatrix}
\tag{44}
$$

where

$$\varepsilon'_j = \frac{-V_{i,j}}{2(\Delta Y)} - \frac{1}{Pr.Re(\Delta Y)^2} \tag{45}$$

$$\beta'_j = \frac{U_{i,j}}{\Delta X} + \frac{2}{Pr.Re(\Delta Y)^2} \tag{46}$$

$$\Omega'_j = \frac{V_{i,j}}{2(\Delta Y)} - \frac{1}{Pr.Re(\Delta Y)^2} \qquad (j>0) \tag{47}$$

$$\Phi'_j = \frac{U_{i,j}\theta_{i,j}}{\Delta X} \tag{48}$$

$$\Omega'_0 = \frac{-2}{Pr.Re(\Delta Y)^2} \qquad (j = 0) \tag{49}$$

For the Constant Heat Flux case, the wall temperature $(\theta_{i+1,n+1})$ is unknown, resulting in $(n+2)$ unknowns. The additional necessary equation (18), which expresses the heat flux at the wall, may be written in difference form as

$$\frac{3\theta_{i+1,n+1} - 4\theta_{i+1,n} + \theta_{i+1,n-1}}{2(\Delta Y)} = 1 \tag{50}$$

The matrix equation (4.14) may be modified to include the additional unknown and equation by adding on an additional row and column.

$$
\begin{vmatrix}
\beta'_0 & \Omega'_0 & & & & & \\
\varepsilon'_1 & \beta'_1 & \Omega'_1 & & & & \\
& \varepsilon'_2 & \beta'_2 & \Omega'_2 & & & \\
& & - & - & - & & \\
& & & - & - & - & \\
& & & & - & - & - \\
& & \varepsilon'_{n-1} & \beta'_{n-1} & & \Omega'_{n-1} & \\
& & & \varepsilon'_n & \beta'_n & & \Omega'_n \\
& & & 1/2(\Delta Y) & -4/2(\Delta Y) & 3/2(\Delta Y) &
\end{vmatrix}
\times
\begin{vmatrix}
\theta_{i+1,0} \\
\theta_{i+1,1} \\
\theta_{i+1,2} \\
- \\
- \\
- \\
\theta_{i+1,n-1} \\
\theta_{i+1,n} \\
\theta_{i+1,n+1}
\end{vmatrix}
=
\begin{vmatrix}
\Phi'_0 \\
\Phi'_1 \\
\Phi'_2 \\
- \\
- \\
- \\
\Phi'_{n-1} \\
\Phi'_n \\
1
\end{vmatrix}
\tag{51}
$$

where the elements are defined as in (44).

The element $1/2(\Delta Y)$ in the last row makes the matrix in (51) nontridiagonal. However, the matrix may be made tridiagonal by eliminating this element. This can be accomplished by dividing the last equation by $1/2(\Delta Y)$, multiplying it by (ε_n), and subtracting the next to the last equation from it. The results are

$$
\begin{vmatrix}
\beta_0' & \Omega_0' & & & & & \\
\varepsilon_1' & \beta_1' & \Omega_1' & & & & \\
 & \varepsilon_2' & \beta_2' & \Omega_2' & & & \\
 & & - & - & - & & \\
 & & & - & - & - & \\
 & & & & - & - & - \\
 & & \varepsilon_{n-1}' & \beta_{n-1}' & & \Omega_{n-1}' & \\
 & & & \varepsilon_n' & \beta_n' & & \Omega_n' \\
 & & & 0 & \left(-4\varepsilon_n' - \beta_n'\right) & \left(3\varepsilon_n' - \Omega_n'\right)
\end{vmatrix}
\times
\begin{vmatrix}
\theta_{i+1,0} \\
\theta_{i+1,1} \\
\theta_{i+1,2} \\
- \\
- \\
- \\
\theta_{i+1,n-1} \\
\theta_{i+1,n} \\
\theta_{i+1,n+1}
\end{vmatrix}
=
\begin{vmatrix}
\Phi_0' \\
\Phi_1' \\
\Phi_2' \\
- \\
- \\
- \\
\Phi_{n-1}' \\
\Phi_n' \\
2(\Delta Y)\varepsilon_n' - \Phi_n'
\end{vmatrix}
\qquad (52)
$$

Calculation of Bulk Temperature

The dimensionless bulk temperature (θ_b) is calculated numerically by employing Simpson's rule:

$$
\theta_b\big|_{i+1} = \frac{\Delta Y}{3}\left(U_{i+1,0}\theta_{i+1,0} + 4\sum_{j=1,3,5,7,\ldots}^{n} U_{i+1,j}\theta_{i+1,j} + 2\sum_{j=2,4,6,8,\ldots}^{n-1} U_{i+1,j}\theta_{i+1,j}\right)
$$

(53)

Equation (53) requires an even number of spaces across the half channel (n must be odd).

Calculation of Local Nusselt Number

The Nusselt number is given by equation (23). The local Nusselt number for Constant Wall Temperature boundary condition is given by equation (27), which is written in a finite difference form as,

$$
N_{ux} = -2\frac{\left(3\theta_{i+1,n+1} - 4\theta_{i+1,n} + \theta_{i+1,n-1}\right)}{2(\Delta Y)\theta_b\big|_{i+1}}
$$

(54)

The local Nusselt number for Constant Heat Flux boundary condition is given by equation (29), which is written in a finite difference form as,

$$
N_{ux} = \frac{-2}{\theta_b\big|_{i+1} - \theta_w\big|_{i+1}}
$$

(55)

Results and Discussion

Results include velocity profile, temperature distribution, bulk temperature, local Nusselt number for two cases of heating Constant Wall Temperature and Constant Heat Flux. The results of the present work are compared with the previous works by [Incropera, 1996] and [Holman, 1999] present in Table (1), (2) and (3).

Development of Velocity Profiles

Figures (1.a), (1.b), (1.c), (1.d) and (1.e) show the velocity profiles which manifest stages of developing the hydrodynamic boundary layer for Reynolds numbers (Re=100), (Re=500), (Re=1000), (Re=1500) and (Re=2000) at different sections of parallel plate channel.

The velocity in the inlet section is uniformly distributed over its width and that its magnitude is ($U=U_o=1$). The velocity at wall equals zero but with an increase distance in y-direction from the surface, the x-direction velocity component of fluid (U), must then increasing until it approaches maximum in centerline of channel. In the fully

developed region the vertical velocity component (V) is zero and the gradient of the axial velocity component $\left(\dfrac{\partial U}{\partial X}\right)$ are everywhere zero.

The velocity profiles become fully developed at approximately $\dfrac{L_e}{2a} = 0.05\,\text{Re}$

The resulting velocity profile consist of two boundary layer profiles on the two walls joined in the center by a line of constant velocity. Since the volume of flow the same for every section, the decrease in the rate of flow near the walls which is due to friction must be compensated by a corresponding increase near the axis.

Temperature Distribution

The dimensionless temperature for Constant Wall Temperature in the inlet section is uniformly distributed over its width and that its magnitude is ($\theta=\theta_o=1$). The dimensionless temperature at the walls equals zero but increases with increasing distance in y-direction from the surface, until it approaches the maximum in the centerline of the channel. The dimensionless temperature for Constant Heat Flux in the inlet section is zero over its width. The dimensionless temperature at the walls equals maximum value but decreases with increasing distance in y-direction from the surface, then it decreases until it approaches minimum in centerline of channel. The temperature distribution becomes fully developed at approximately $\dfrac{L_{et}}{2a} = 0.05\,\text{Re}.\text{Pr}$. In the fully developed region the gradient of the dimensionless temperature $\left(\dfrac{\partial \theta}{\partial X}\right)$, is everywhere zero because of the reaching of the fluid temperature to a value close to the wall temperature.

Prandtl number effected on the shape of the dimensionless temperature distribution. The Prandtl number is given by $\text{Pr} = \dfrac{\nu}{\alpha}$. It is a ratio of kinematic viscosity to thermal diffusivity. Physically, it relates the viscous effects to the thermal effects. When ($\text{Pr} > 1.0$) then ($\nu > \alpha$) and a momentum disturbance propagates farther into the free stream than a thermal disturbance.

Overall Heating

Maximum dimensionless bulk temperature for Constant Wall Temperature equals to (0.94) at the first step and decreases this value with increasing the axial distance from inlet. Minimum dimensionless bulk temperature for Constant Heat Flux approximately equals to zero in the first step and increases with increasing axial distance from inlet and reaches maximum value of approximately (0.091). For low Prandtl number the dimensionless bulk temperature is faster the reach to the minimum value (for Constant Wall Temperature) or maximum value (for Constant Heat Flux) because small thermal entry length and the reverse is true for high Prandtl number. The dimensionless bulk temperature (dimensionless mean temperature) depends on Prandtl, Reynolds number, and the axial distance (X).

Local Nusselt Number

Nusselt number has the maximum value at the start of entrance region (first step) and then decreases gradually until it will be close to thermal fully developed region. The boundary layer thickness is zero at the start of entrance region, hence, there is no resistance against heat transfer which leads to raise the heat transfer coefficient value to maximum. So the heat transfer coefficient decreases when the boundary layer begins the process of developing until it reaches a constant value. The length at which

the thermal boundary layer is fully developed increases with increasing Reynolds and Prandtl numbers.

It is noted that the local Nusselt number for the Constant Heat Flux case is greater than the local Nusselt number for Constant Wall Temperature case, however, the flow field is similar for all studied cases (same Reynolds and Prandtl numbers). The local Nusselt number changes along the length of the channel, this is confirmed by the result shown in figures (from (5-41) to (5-48)). Results of this numerical procedure appear to be in a close agreement with the correlation related to it [Incropera, 1996] and [Holman, 1999].

CONCLUSIONS

The maximum velocity at the centerline of the channel, in the fully developed region the vertical velocity component (V) is zero and the gradient of the axial velocity component ($\partial U/\partial X$) are everywhere zero, hence, the axial velocity component depends only on (Y). It can be seen that the boundary layer developed faster for the lower Reynolds number. However, the flow field is similar for all studied cases. At fully developed region the shape of velocity profile becomes parabolic over the width of the channel. The velocity profile becomes fully developed at approximately $\frac{L_e}{2a} = 0.05\,\mathrm{Re}$. The maximum dimensionless temperature for constant wall temperature at the centerline of the channel but for constant wall heat flux boundary condition is at the walls. The thermal boundary layer developed faster for lower Reynolds and Prandtl numbers, however, the flow field is similar to the studied cases. The dimensionless temperature distribution becomes fully developed at approximately $\frac{L_{et}}{2a} = 0.05\,\mathrm{Re}.\mathrm{Pr}$. If (Pr > 1), the hydrodynamic boundary layer develops more rapidly than the thermal boundary layer ($L_e < L_{et}$), while inverse is true (Pr < 1), but if (Pr = 1) the hydrodynamic and thermal boundary layers are the same ($L_e = L_{et}$). The Nusselt number has the maximum value at the start of entrance region (first step) and then decreases gradually until it will be close to thermal fully developed region, because of the high velocities near the walls at the entrance and decreases these velocities with an axial direction. The Nusselt number of constant wall heat flux boundary condition greater is than Nusselt number for constant wall temperature boundary condition case, however, the flow field is similar for all studied cases.

REFERENCES

[1] **Muzychka, Y.S. and Yovanovich, M.M.** "Laminar Forced Convection Heat Transfer in the Combined Entry Region of Non-Circular Ducts", ASME Journal of Heat Transfer, Vol. 126, pp. 54-61., 2004

[2] **Lawal, A.** "Mixed Convection Heat Transfer to Power Law Fluids in Arbitrary Cross-Sectional Ducts", J. Heat Transfer, Vol. 111, pp. 399-406., 1989

[3] **Al-Ali, H.H. and Selim, M.S.** "Momentum and Heat Transfer in the Entrance Region of a parallel plate channel: Developing Laminar Flow with constant wall temperature", Int. J. Heat Mass Transfer, Vol. 51, No. 4, 1992

[4] **Lakovic, S., Stefanovic, V., Ilic, G., and Stojiljkovic, M.** "Convective Heat and Mass Transfer under the Conditions of Hydrodynamic Stabilization of the Flow", Int.

J. The Scientific Journal FACTA UNIVERSITATIS,   Vol. 1, No. 4, pp. 397-407., 1997

[5] Silva, E.F., Guerrero, J.S., and Cotta, R.M. "Integral transform solution of boundary layer equations in stream function-only formulation", Int. J. of NON-LINEAR MECHANICS, Vol. 34, pp. 51-61., 1999

[6] Adachi, T. and Uehara, H. "Correlation between heat transfer and pressure drop in channels with periodically grooved parts", Int. J. Heat and Mass Transfer, Vol. 44, pp. 4333-4343, 2001., 2001

[7] Barber, R.W. and Emerson, D.R. "The influence of Knudsen number on the hydrodynamic development length within parallel plate micro-channels", E-mail: r.w.barber@dl.ac.uk, Web page: http://www.cse.clrc.ac.uk/Group/CSECEG., 2002

[8] Hornbeck, R.W. "Numerical Marching Techniques for Fluid Flows with Heat Transfer", National Aeronautics and Space Administration, Washington., 1973

[9] Incropera, F.P. and Dewitt, D.P. "Fundamentals of Heat and Mass Transfer", John Wiley & Sons, New York., 1996

[10] Adams, J.A. and Rogers D.F. "Computer-Aided Heat Transfer Analysis", McGraw-Hill Book Company, New York., 1973

[11] Schlichting, H. "Boundary-Layer Theory", McGraw-Hill Book Company, New York., 1968

[12] Anderson, D.A., Tannehill, J.C., and Pletcher, R.H. "Computational Fluid Mechanics and Heat Transfer", McGraw-Hill Book Company, New York., 1984

[13] Holman, J.P. "Heat Transfer", McGraw-Hill Book Company, New York., 1999

NOMENCLEATURE:

Symbol	Definition	Unit
a	The Distance Between Centerline and Wall of Duct	m
C.H.F	Constant Heat Flux	——
C.W.T	Constant Wall Temperature	——
d	The Distance Between Two Parallel Plate Channel	m
D	Diameter of Circular Duct	m
h	Heat Transfer Coefficient	W/m2K
k	Thermal Conductivity	W/mK
L	Length of Channel	m
Le	Hydrodynamic Entry Length	m
Let	Thermal Entry Length	m
m	Number of Grid Nodes in the Axial Direction	——
n	Number of Grid Nodes in the Vertical Direction	——
Nu	Nusselt Number	——
Nux	Local Nusselt Number	——
p	Pressure	N/m2

P	Dimensionless Pressure	——
Pr	Prandtl Number	——
Q	Heat Transfer Rate	W
qs"	Heat Flux	W/m2
r	Radial Direction of Circular Duct	m
Re	Reynolds Number	——
T	Temperature	^{o}c
Tb	Bulk Temperature	^{o}c
θ	Dimensionless Temperature	——
θb	Dimensionless Bulk Temperature	——
u	Velocity in Axial Direction	m/s
U	Dimensionless Velocity in Axial Direction	——
v	Velocity in Vertical Direction	m/s
V	Dimensionless Velocity in Vertical Direction	——
x	Axial Direction of the Duct	m
X	Dimensionless Axial Direction of the Duct	——
Δx	The Distance Between Two Nodal Points in the Axial Direction	m
ΔX	The Dimensionless Distance Between Two Nodal Points in the Axial Direction	——
y	Vertical Direction of the Duct	m
Y	Dimensionless Vertical Direction of the Duct	——
Δy	The Distance Between Two Nodal Points in the Vertical Direction	m
ΔY	The Dimensionless Distance Between Two Nodal Points in the Vertical Direction	——
Greek Symbols		
A	Thermal Diffusivity	m2/s
N	Kinematic Viscosity	m2/s
M	Dynamic Viscosity	N.s/m2
P	Density of Fluid	kg/m3
Cp	Specific Heat at Constant Pressure	J/kg.K
Δ	Hydrodynamic Boundary Layer Thickness	m
δ t	Thermal Boundary Layer Thickness	m
Subsxripts		
i, j	The Index Increment Along the Axial and Vertical Direction	——
o	Inlet	——
w	Refers to Wall	——
s1	Refers to First Surface	——
s2	Refers to Second Surface	——

Table (1) Comparison the hydrodynamic entry length with previous work

	hydrodynamic entry length (L_e)
Incropera	L_e =0.05 D Re
Holman	L_e =0.05 D Re
Present work	L_e =0.05 d Re

Table (2) Comparison the thermal entry length with previous work

	thermal entry length (L_{et})
Incropera	L_{et} =0.05 D Pr Re
Holman	L_{et} =0.05 D Pr Re
Present work	L_{et} =0.05 d Pr Re

Table (3) Comparison the Nusselt number with previous work

	Nusselt number (Nu)			
	Maximum value		Minimum value	
	C.W.T	C.H.F	C.W.T	C.H.F
Incropera	13	14.8	3.66	4.36
Holman	12.8	14.6	3.66	4.364
Present work	12.8	18	4.3	5.1
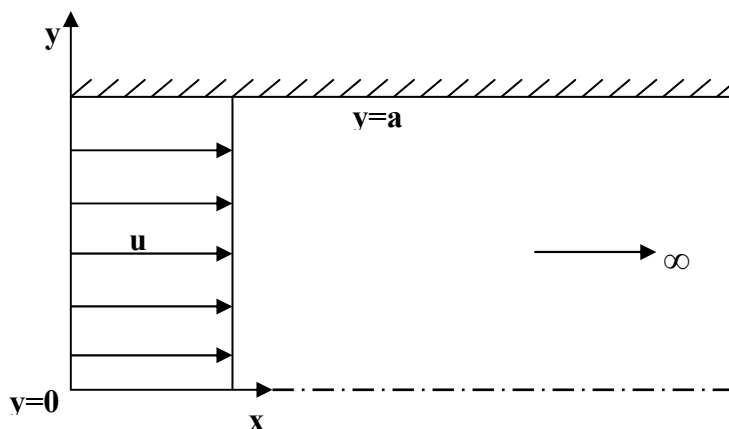
Fig. (1): Problem Configuration and Coordinate System for Parallel Plate Channel
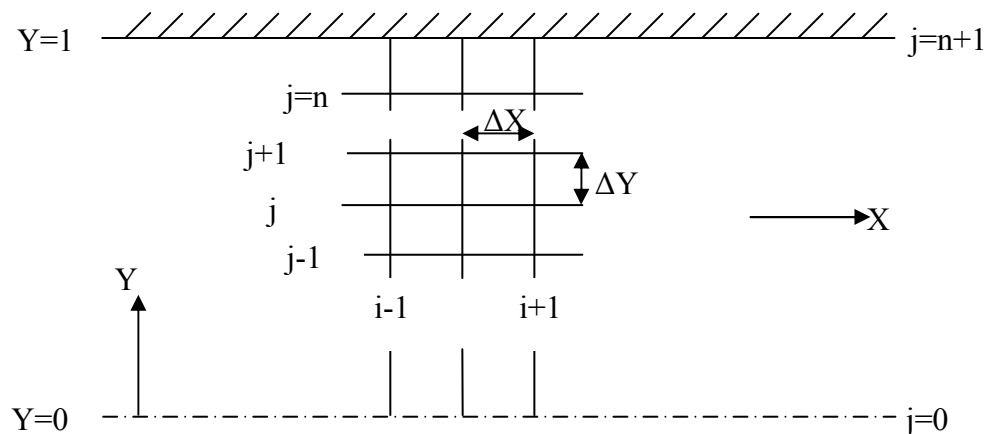
Fig. (2): Finite Difference Grid For Parallel Plate Channel
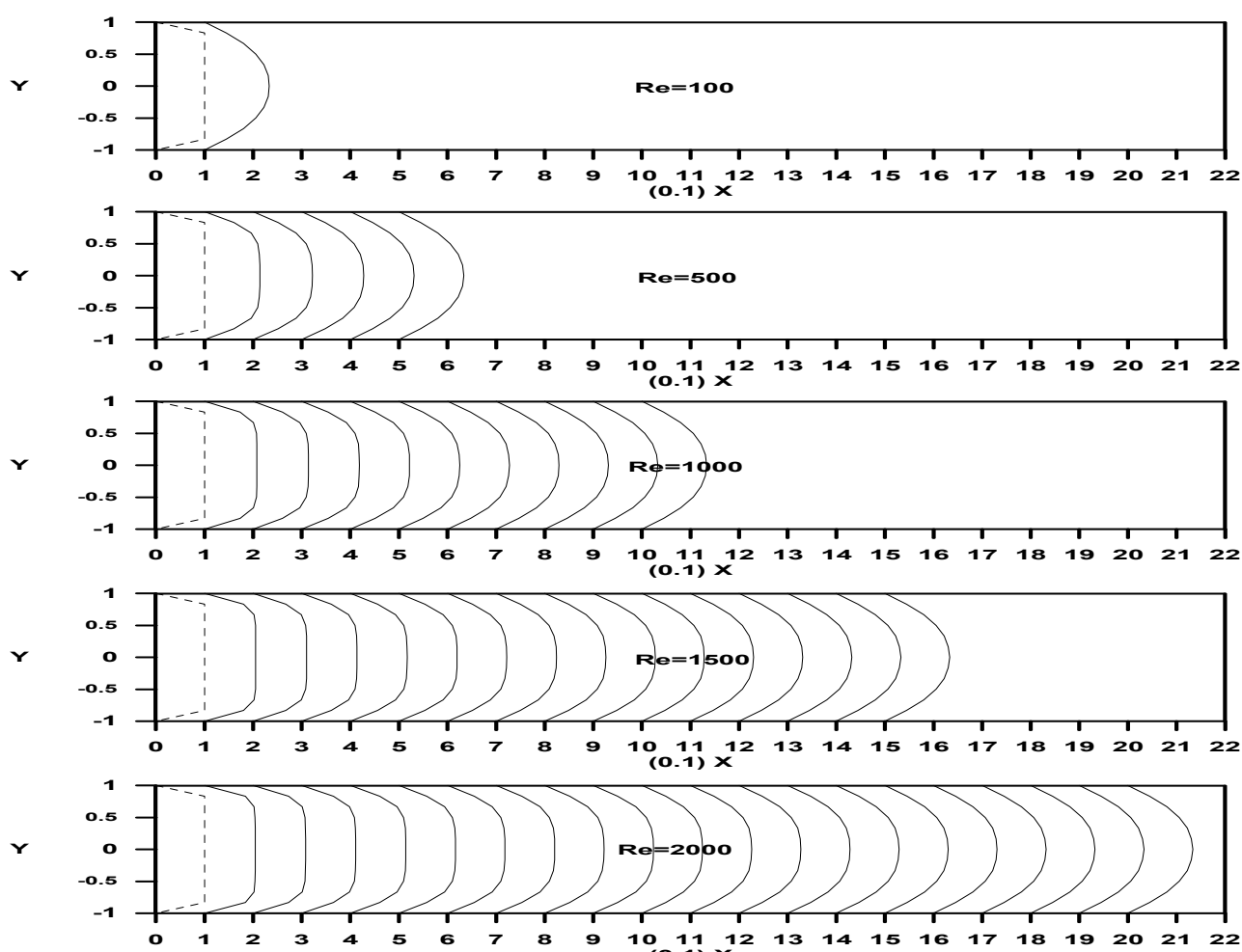
Fig. (3) Laminar, hydrodynamic velocity profile development in a parallel plate channel for different Reynolds number
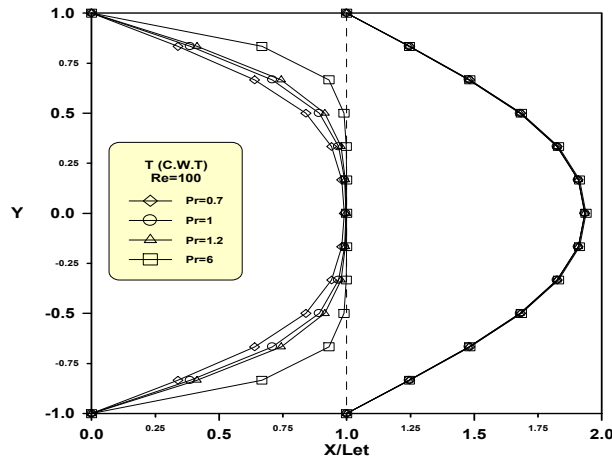
Fig.(4) Developing and fully developed temperature distribution in a parallel plate channel for constant wall temperature, Re=100, different Prandtl number
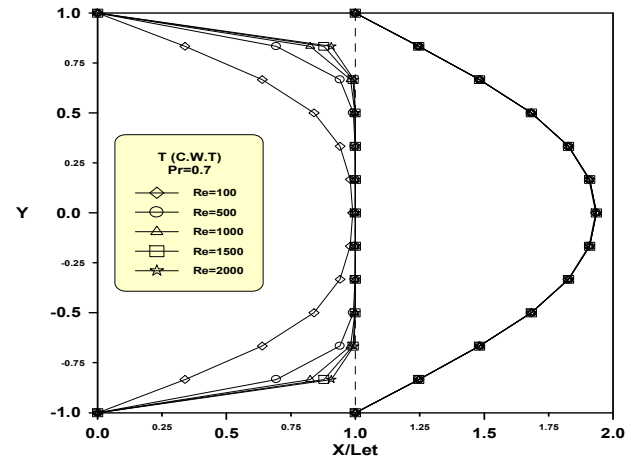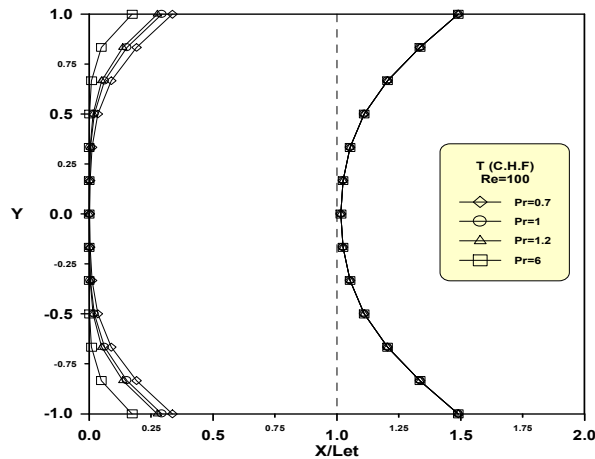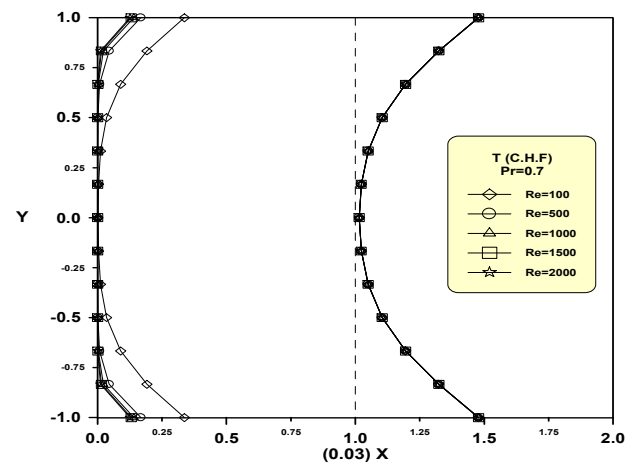

Fig.(5) Developing and fully developed temperature distribution in a parallel plate channel for constant wall temperature, Pr=0.7, different Reynolds number

Figure (6) Developing and fully developed temperature distribution in a parallel plate channel for constant heat flux, Re=100, different Prandtl number

Figure (7) Developing and fully developed temperature distribution in a parallel plate channel for constant heat flux, Pr=0.7, different Reynolds number
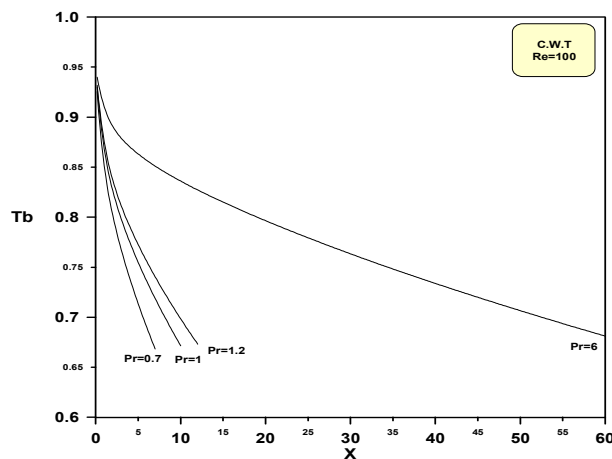
Fig.(8) Bulk temperature in a parallel plate channel for constant wall temperature, Re=100, different Prandtl number
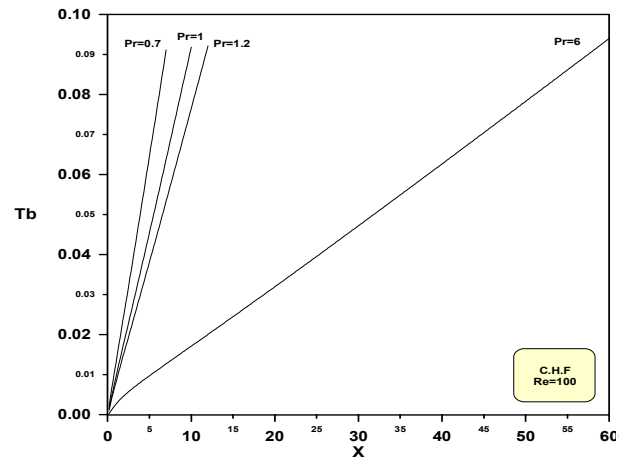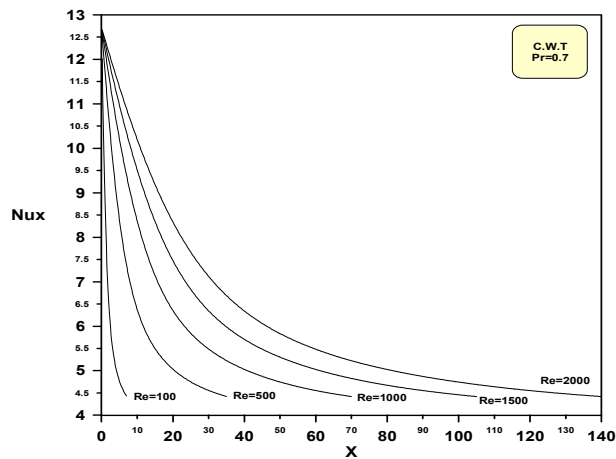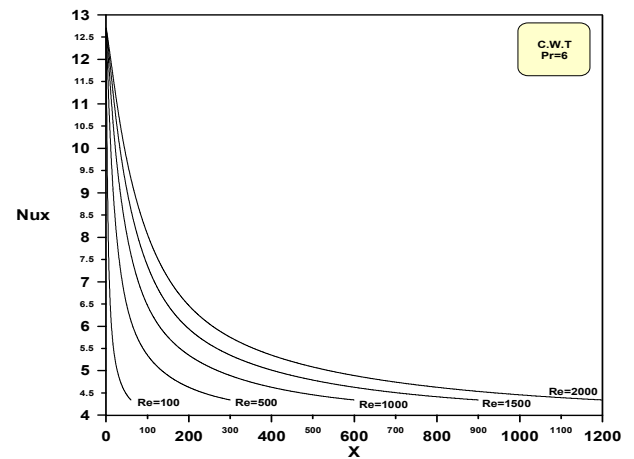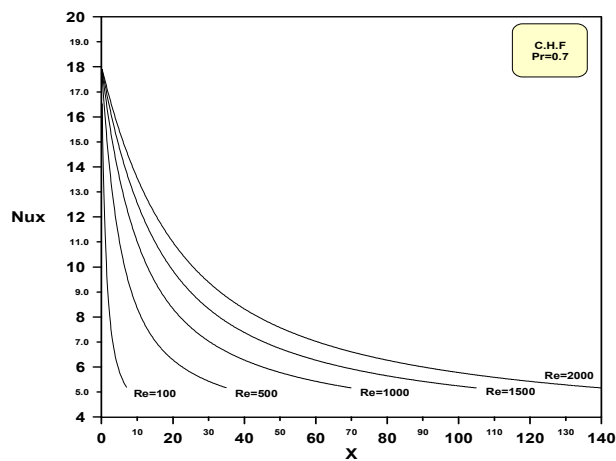

Fig.(9) Bulk temperature in a parallel plate channel for constant heat flux, Re=100, different Prandtl number

41
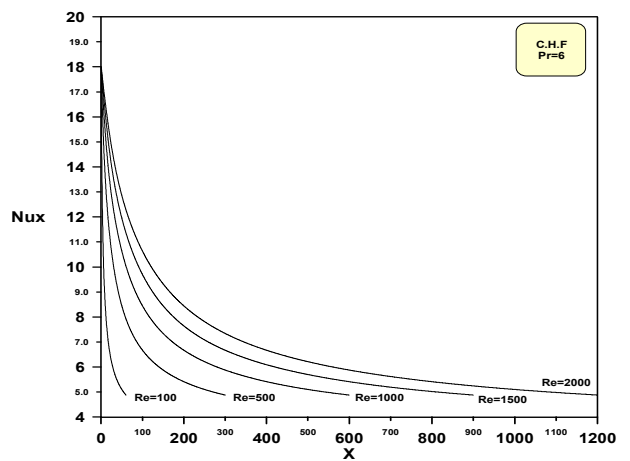
Fig.(10) Local Nusselt number in a parallel plate channel for constant wall temperature, **Pr=0.7**, different Revnolds number

Fig.(11) Local Nusselt number in a parallel plate channel for constant wall temperature, **Pr=6**, different Reynolds number

Fig.(12) Local Nusselt number in a parallel plate channel for constant heat flux, **Pr=0.7**, different Revnolds number

Fig.(13) Local Nusselt number in a parallel plate channel for constant heat flux, **Pr=6**, different Reynolds number